Oncogene (2009) 28, 363–377

www.nature.com/onc

ORIGINAL ARTICLE

Annexin A6 inhibits Ras signalling in breast cancer cells

S Vilà de Muga[1], P Timpson[2], L Cubells[1], R Evans[3], TE Hayes[3], C Rentero[1], A Hegemann[3], M Reverter[1], J Leschner[3], A Pol[4], F Tebar[1], RJ Daly[2], C Enrich[1,4] and T Grewal[3]

[1]Departament de Biologia Cel·lular, Facultat de Medicina, Universitat de Barcelona, Barcelona, Spain; [2]The Garvan Institute of Medical Research, Sydney, NSW, Australia; [3]Faculty of Pharmacy, University of Sydney, Sydney, Australia and [4]Institut d'Investigacions Biomèdiques August Pi i Sunyer (IDIBAPS), Facultat de Medicina, Universitat de Barcelona, Barcelona, Spain

Overexpression of epidermal growth factor receptor (EGFR) is associated with enhanced activation of wild-type (hyperactive) Ras in breast cancer. Little is known about the regulation of Ras inactivation and GTPase-activating proteins (GAPs), such as p120GAP, in cells with hyperactive Ras. Recently, we showed that in EGFR-overexpressing A431 cells, which lack endogenous Annexin A6 (AnxA6), ectopic expression of AnxA6 stimulates membrane recruitment of p120GAP to modulate Ras signalling. We now demonstrate that, AnxA6 is downregulated in a number of EGFR-overexpressing and estrogen receptor (ER)-negative breast cancer cells. In these cells, AnxA6 overexpression promotes Ca^{2+}- and EGF-inducible membrane targeting of p120GAP. In ER-negative MDA-MB-436 cells, overexpression of p120GAP, but not CAPRI or a p120GAP mutant lacking the AnxA6-binding domain inhibits Ras/MAPK activity. AnxA6 knockdown in MDA-MB-436 increases Ras activity and cell proliferation in anchorage-independent growth assays. Furthermore, AnxA6 co-immunoprecipitates with H-Ras in a Ca^{2+}- and EGF-inducible manner and fluorescence resonance energy transfer (FRET) microscopy confirmed that AnxA6 is in close proximity of active (G12V), but not inactive (S17N) H-Ras. Thus, association of AnxA6 with H-Ras-containing protein complexes may contribute to regulate p120GAP/Ras assembly in EGFR-overexpressing and ER-negative breast cancer cells.

Oncogene (2009) **28,** 363–377; doi:10.1038/onc.2008.386; published online 13 October 2008

Keywords: Annexin A6; p120GAP; Ras; EGF receptor; breast cancer

Introduction

In mammalian cells, the epidermal growth factor receptor (EGFR)/Ras/mitogen-activated protein kinase (MAPK) pathway is an important signal-transducing module involved in the development of cancer. At the cell surface, binding of EGF to the EGFR leads to the activation of Ras, which then recruits Raf and MAPK to propagate the signal. Ras inactivation is regulated by GTPase-activating proteins (GAPs), which accelerate the hydrolysis of GTP-bound Ras. Oncogenic Ras (G12V, Q61L) cannot be switched off by GAPs and remains constitutively active. In addition, enhanced wild-type Ras activity because of increased coupling to overexpressed EGFR or loss of GAP activity can contribute to cell transformation in breast and numerous other cancers (Malaney and Daly, 2001; Cook and Lockyer, 2006; Cullen, 2006; Grewal and Enrich, 2006).

Plasma membrane targeting of GAPs is facilitated by SH2, SH3, PH and Ca^{2+}-dependent phospholipid-binding (CaLB/C2) domains. CAPRI, RASAL, p120GAP, require the CaLB/C2 domain for membrane association (Davis *et al*., 1996; Lockyer *et al*., 2001; Walker *et al*., 2004; Grewal and Enrich, 2006; Pena *et al*., 2008). On Ca^{2+} increase, p120GAP, CAPRI and RASAL are rapidly recruited to the plasma membrane to inhibit Ras, but in contrast to CAPRI and RASAL, the C2 domains of p120GAP cannot bind Ca^{2+} (Walker *et al*., 2003; Grewal and Enrich, 2006). However, we and others identified that AnxA6, a Ca^{2+}-dependent membrane-binding protein, binds to the CaLB/C2 domain and targets p120GAP to the plasma membrane in a Ca^{2+}-dependent manner (Davis *et al*., 1996; Grewal *et al*., 2005; Rual *et al*., 2005).

Out of the divergent GAP protein family it is unclear which GAP contributes to downregulate EGFR-induced Ras signalling. p120GAP is expressed ubiquitously and the only GAP known to bind EGFR (Cooper and Kashishian, 1993; Wang *et al*., 1996; Jones *et al*., 2006). Overexpression of p120GAP suppresses Ras-dependent transformation (Zhang *et al*., 1990; Nori *et al*., 1991) and membrane-anchoring of p120GAP potentiates Ras inactivation (Huang *et al*., 1993). In contrast, inhibiting p120GAP binding to EGFR increases Ras activity (Agazie and Hayman, 2003) and p120GAP ko-cells exhibit hyperactive Ras and sustained MAPK activity (van der Geer *et al*., 1997).

Accumulating evidence points at AnxA6 facilitating p120GAP-mediated inactivation of EGFR-induced Ras signalling. AnxA6 is found in activated EGFR protein complexes (Blagoev *et al*., 2003) and in several cancer

Correspondence: Dr T Grewal, Faculty of Pharmacy A15, University of Sydney, Sydney, NSW 2006, Australia.
E-mail: tgrewal@pharm.usyd.edu.au or Dr C Enrich, Departament de Biologia Cellular, Facultat de Medicina, Universitat de Barcelona, Casanova 143, Barcelona 08036, Spain.
E-mail: enrich@ub.edu
Received 16 July 2008; revised 15 September 2008; accepted 15 September 2008; published online 13 October 2008

models loss of AnxA6 expression correlates with elevated EGFR/Ras activity (Grewal and Enrich, 2006). A431 cells, a vulval squamous epithelial carcinoma cell line, which overexpress the EGFR and show elevated Ras/MAPK activity, lack endogenous AnxA6 (Smythe *et al*., 1994; Grewal *et al*., 2005). Restoration of AnxA6 expression in A431 cells stimulates the Ca^{2+}-dependent membrane recruitment of p120GAP and inhibits EGF-induced Ras activity. Importantly, RNAi-mediated p120GAP knockdown enhanced Ras activity more strongly in AnxA6-expressing A431 (A431anx6) cells than controls, suggesting the increased involvement of p120GAP in Ras inactivation in A431anx6 cells (Grewal *et al*., 2005; Rentero *et al*., 2006).

Previous studies addressing the role of p120GAP in EGFR/Ras inactivation almost exclusively utilized cell lines or p120GAP ko-MEFs with low EGFR levels (Zhang *et al*., 1990; Nori *et al*., 1991; Cooper and Kashishian, 1993; Huang *et al*., 1993; Wang *et al*., 1996; van der Geer *et al*., 1997). Yet little is known about the regulation of p120GAP in cells overexpressing EGFR and hyperactive Ras. Our findings in A431 cells prompted us to analyse AnxA6 and p120GAP expression in breast cancer cells (BCCs), which often contain hyperactive Ras because of increased coupling to overexpressed/deregulated members of the EGFR family (Malaney and Daly, 2001). Although p120GAP is expressed similarly in all cell lines analysed, AnxA6 levels are strongly reduced in EGFR overexpressing and several other ER-negative BCCs. Ectopic expression of AnxA6 in EGFR-overexpressing BCCs promotes p120GAP membrane targeting, downregulates Ras activity, mitogenic signalling and reduces cell growth. Co-immunoprecipitations and FRET microscopy suggest that AnxA6 interacts with active H-Ras (HRasG12V), but not inactive H-Ras (HRasS17N) in an EGF- and Ca^{2+}-inducible manner, indicating that AnxA6 is part of a protein complex stabilizing Ras/p120GAP assembly.

Results

Reduced AnxA6 expression levels in EGFR overexpressing and ER-negative BCCs

To address a possible correlation between EGFR/ErbB2, AnxA6 expression and Ras activity in BCCs, we first analysed AnxA6 and p120GAP protein levels in well-characterized BCCs (deFazio *et al*., 2000; Daly *et al*., 2002) (Figure 1a). Whereas p120GAP is expressed similarly, AnxA6 expression differs significantly when comparing ER-positive and ER-negative BCCs. BCCs with deregulated ErbB2/3 (lanes 3–8; lanes 4, 5 and 8 correspond to ER-positive lines) and all ER-positive BCCs (lanes 18–21) express high levels of AnxA6 ($\sim$3–5 pg per cell). In contrast, 6 out of 12 ER-negative lines display low AnxA6 levels, and all of these have moderate to high EGFR overexpression (deFazio *et al*., 2000). In particular, similar to A431, BCCs with EGFR amplification (lanes 9, 10: BT20, MDA-MB-468) exhibit very low AnxA6 levels ($<$1 pg per cell; (Cubells *et al*., 2007)). Hence downregulation of AnxA6 could be linked to hyperactive Ras activity in EGFR-overexpressing BCCs.

To identify if AnxA6 stimulates p120GAP translocation in EGFR-overexpressing BCCs, membranes from MDA-MB-468 and BT20 controls and stable cell lines overexpressing AnxA6 (MDA-MB-468anx6, BT20anx6) incubated ± EGF (10 ng/ml) or Ionomycin (2 μM) were isolated (Jaumot and Hancock, 2001) and analysed for membrane-bound p120GAP and AnxA6 (Figure 1b). p120GAP was not detectable in membranes of unstimulated MDA-MB-468 controls (lane 1). Stimulation with Ca^{2+} or EGF slightly increased the membrane-bound p120GAP in these cells (lanes 2–3). In contrast, in MDA-MB-468anx6 the p120GAP membrane association increased 7- to 10-fold upon Ca^{2+} or EGF stimulation (lanes 4–6, see quantification in Figure 1b). In BT20 controls, only EGF, but not Ionomycin, increased membrane binding of p120GAP. In contrast, BT20anx6 cells exhibited increased levels of membrane-associated p120GAP even in the absence of Ca^{2+} (Figure 1b, lanes 10–12). Furthermore, Ionomycin induced a strong increase of membrane-bound p120GAP in BT20anx6, but not BT20wt (compare lanes 9 and 12). Thus, high AnxA6 levels correlate with increased EGF- and Ca^{2+}-inducible membrane translocation of p120GAP in EGFR-overexpressing BCCs.

Similar to the results obtained for p120GAP in MDA-MB-468 and BT20 controls, small amounts of endogenous AnxA6 are only detectable in membranes of Ionomycin-treated MDA-MB-468 (lane 3). In MDA-MB-468anx6, both EGF and Ionomycin promoted AnxA6 membrane translocation (lanes 5–6). BT20anx6 cells are characterized by large amounts of membrane-bound AnxA6 even in the absence of EGF or Ca^{2+} (lanes 10–12), which might reflect substantial amounts of the membrane-associated and Ca^{2+}-independent pool of AnxA6 proteins also in BT20 cells (de Diego *et al*., 2002). Taken together, these findings indicate that either cytosolic AnxA6 is targeted to the plasma membrane together with p120GAP or possibly serves as a membrane-bound docking site for p120GAP.

Annexin A6 promotes Ras inactivation in EGFR-overexpressing BCCs

We then compared Ras/MAPK activity in BT20 cells ± ectopically expressed AnxA6 (Figure 2a). Activation of Ras and Mek1/2 in response to EGF was reduced by $\sim$40–50 and 25–40% in BT20 cells overexpressing AnxA6, respectively (compare lanes 2 and 4). Similar results were obtained in a stable cell line expressing AnxA6 (BT20anx6) and in transiently transfected MDA-MB-468 (data not shown). Ras activity was also inhibited by more than 50% in BT20 cells stably expressing the AnxA6 fragment $AnxA6_{1-352}$ (Figure 2b; compare lanes 6 and 10) which comprises the first four AnxA6 membrane-binding repeats and the linker region to bind p120GAP (Grewal T and Enrich C, unpublished results). In contrast, stable expression of

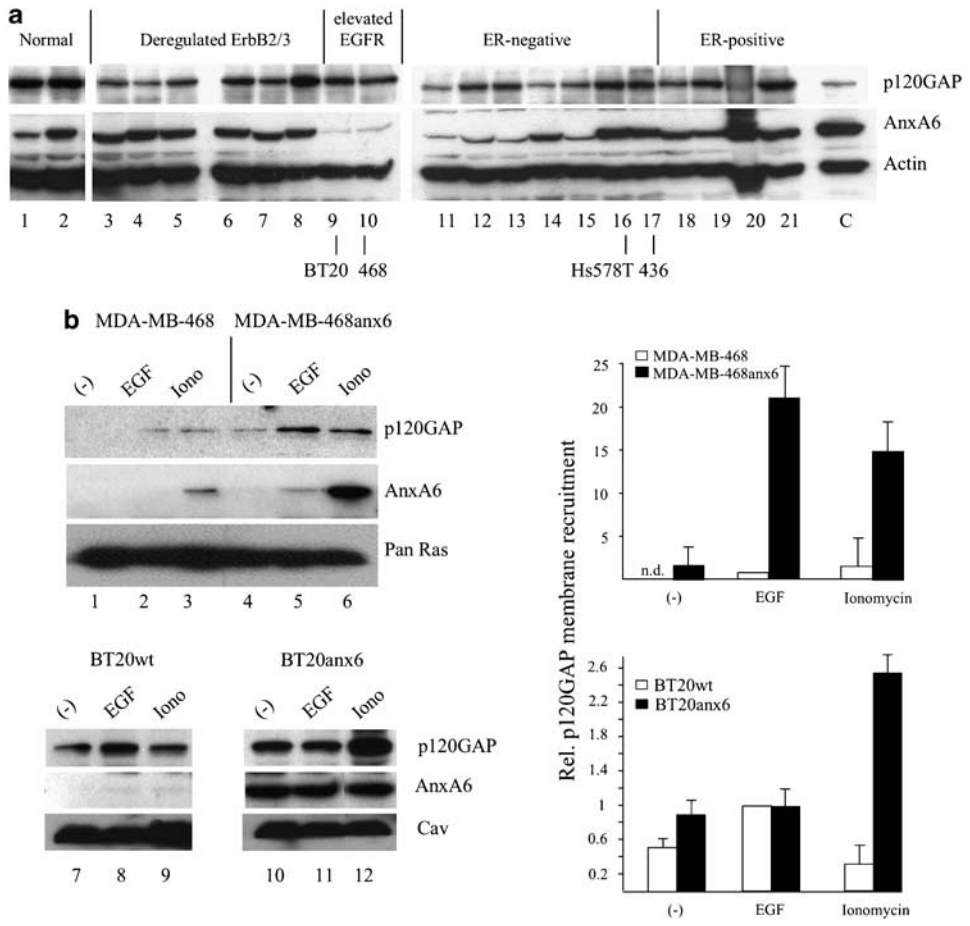

Figure 1 AnxA6 expression in breast cancer cells (BCC). (**a**) p120GAP, AnxA6 and actin expression levels in normal breast epithelial cell strains (lanes 1, 2: 184AI, HMEC-219-4), breast cancer cell lines (BCCs) with elevated ErbB2/3 (lanes 3–8: MDA-MB-453, BT474, MDA-MB-175, SKBR3, MDA-MB-361, ZR75-1), estrogen receptor (ER) -negative BCCs with elevated EGFR (lanes 9, 10: BT20, MDA-MB-468), ER-negative BCCs (lanes 11–17: HBL-100, MDA-MB-231, BT549, MDA-MB-330, MDA-MB-157, Hs578T, MDA-MB-436), ER-positive BCCs (lanes 18–21: T47D, MCF-7, MDA-MB-134, BT483) and A431anx6 cells (C, control). (**b**) MDA-MB-468 (lanes 1–3), MDA-MB-468anx6 cells (lanes 4–6), BT20wt (lanes 7–9) and BT20anx6 (lanes 10–12) were incubated ± EGF (10 ng/ml) or Ionomycin (2 μM). Crude membranes and cytosol were isolated and incubated for 30 min at 30 °C. Membranes were re-isolated by ultracentrifugation and the membrane-bound proteins were analysed by western blotting for p120GAP, AnxA6, Pan Ras and caveolin (Cav) as indicated. Relative levels of membrane-bound p120GAP in MDA-MB-468, BT20wt controls (white bars), MDA-MB-468anx6 and BT20anx6 cells (black bars) from three independent experiments were quantified and normalized to Pan Ras (lanes 1–6) and to caveolin levels (lanes 7–12). The mean values (± s.d.; nd; not detectable) are shown.

the cytosolic N-terminal mutant $AnxA6_{1-175}$, (lane 3) which cannot bind p120GAP (Pons *et al*., 2001a, b; Grewal *et al*., 2005) did not inhibit EGF-induced Ras activity (Figure 2b, compare lanes 6 and 8).

To address if AnxA6 inhibits Ras in EGFR-overexpressing cells in a Ca^{2+}-dependent manner, we pre-incubated A431anx6 and A431wt cells with a Ca^{2+}-ionophore and compared EGF-induced Ras activity as described previously (Grewal *et al*., 2005) (Figure 3a). Similar to previous results, AnxA6 strongly inhibits EGF-induced Ras activity (~50%; compare lanes 1, 2 and 5, 6). Incubation with Ionomycin alone did not affect basal Ras activity in both cell lines (compare lanes 1 and 4 and 5 and 8). However, pre-incubation of A431anx6, but not A431wt, with Ionomycin resulted in a complete inhibition of EGF-induced Ras activity (compare lanes 2, 3 and 6, 7; for quantification see Figure 3a).

We then compared EGF-induced Ras activity in MDA-MB-468 transfected with AnxA6 that were pre-incubated with or without BAPTA-AM a Ca^{2+}-chelator, followed by EGF activation (Figure 3b). Overexpression of AnxA6 in MDA-MB-468 strongly reduced EGF-induced Ras activity (~60–70%). Importantly, pre-incubation with BAPTA-AM reverted the inhibitory effect of AnxA6 on Ras (Figure 3b, compare lanes 3 and 4) activity, supporting a model of AnxA6 inhibiting Ras through Ca^{2+}-dependent mechanisms. In agreement with the reduced Ca^{2+}-sensitivity of AnxA6 membrane recruitment in BT20anx6 (Figure 1b), AnxA6 inhibited EGF-induced Ras activity by ~50% (Figure 3b), but BAPTA-AM pre-treatment only had a minor effect on the inhibitory activity of AnxA6 on Ras-GTP levels in these cells (compare lanes 6–8).

To determine the specificity of p120GAP in Ras inactivation and its dependence on AnxA6 in

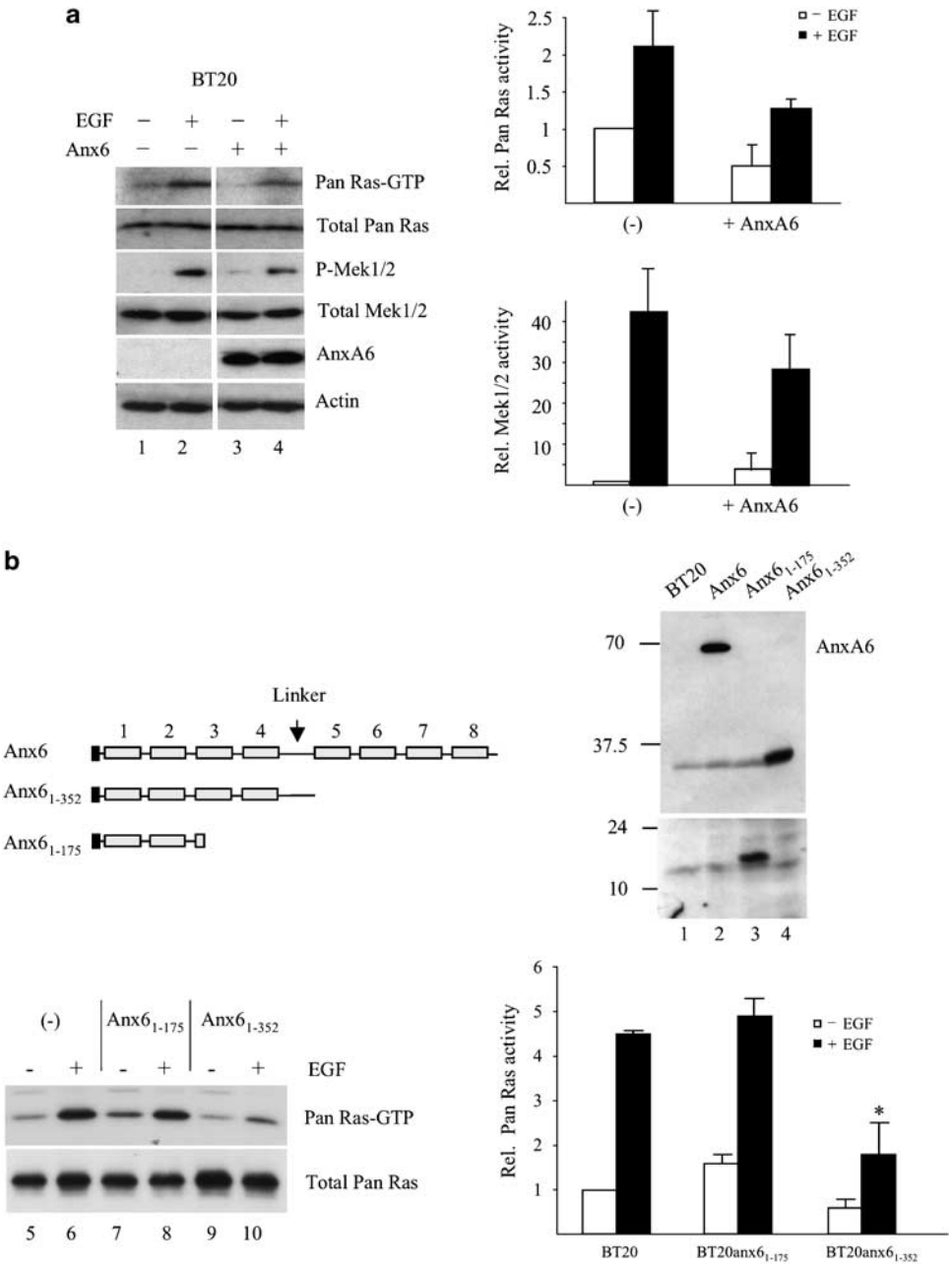

Figure 2 AnxA6 inhibits EGF-induced Ras signalling in BT20 cells. (**a**) EGF receptor overexpressing BT20 wildtype (BT20) were transfected with empty control (−) or AnxA6 expression vector (+). Then 24 h after transfection, cells were starved overnight (ON) and incubated with EGF (10 ng/ml) for 3 min as indicated. Lysates were subjected to RBD pulldowns to determine activated Ras (Pan Ras-GTP) levels. Total Ras, Total Mek1/2, MAPK activation (P-Mek1/2), AnxA6 and actin expression in each lysate is shown. Western blots of three independent Ras and Mek1/2 activation experiments were quantified and normalized to the amounts of Total Pan Ras and Total Mek1/2. The mean values (± s.d.) of the relative Pan Ras and Mek1/2 activity are shown. (**b**) Stable BT20 cell lines expressing N-terminal 37 kDa deletion mutants AnxA6$_{1-352}$ (four AnxA6 repeats plus the AnxA6 linker, see lane 4) and 18 kDa AnxA6$_{1-175}$ (two AnxA6 repeats, see lane 3) were starved ON and incubated ± EGF (10 ng/ml) for 3 min as indicated. Lysates were subjected to RBD pulldowns to determine activated Ras (Pan Ras-GTP) levels (lanes 5–10). Total Ras in each lysate is shown. Western blots of four independent Ras activation experiments were quantified, normalized to the amounts of Total Pan Ras and the mean values (± s.d.) of the relative Pan Ras activity are shown. $^*P<0.05$ for Student's *t*-test.

ER-negative BCCs, we transfected MDA-MB-436, which express high levels of AnxA6 (see lane 17 in Figure 1a), with full-length p120GAP, a p120GAP mutant lacking the 43 amino acid CaLB/C2 domain (p120GAPΔC2) that binds AnxA6 (Gawler *et al*., 1995; Davis *et al*., 1996; Chow and Gawler, 1999) and CAPRI (Figure 3c). Compared with controls, p120GAP overexpression resulted in a 40–50% (Pan Ras-GTP) and 75–85% (H-Ras-GTP) reduction of EGF-stimulated Ras activity (compare lanes 1, 2 and 5, 6). Interestingly,

overexpression of CAPRI did not inhibit Pan Ras, Mek1/2 and Erk1/2 activity and only modestly reduced EGF-induced H-Ras-GTP levels (compare lanes 1, 2 and 3, 4). Together with the low expression levels of CAPRI in ER-negative BCCs (Grewal T, Enrich C, Cullen PJ and Lockyer PJ, unpublished results) and the recently identified Rap-GAP activity of CAPRI (Kupzig *et al*., 2006), these results suggest that CAPRI does not play a prominent role in the downregulation of EGFR-induced Ras signalling. On the other hand, overexpression of the p120GAPΔC2 mutant reduced Pan and H-Ras activity by only ~15 and 50%, respectively (Figure 3c, compare lanes 1, 2 and 7, 8). Furthermore, only full-length p120GAP, but not the p120GAPΔC2 mutant inhibited Mek1/2 and Erk1/2 phosphorylation by ~40–50%. (compare lanes 2 and 8). Thus the loss of AnxA6 binding appears responsible for the inability of the p120GAPΔC2 mutant to inactivate the Ras/MAPK pathway.

We then examined whether AnxA6 knockdown could increase Ras activity in ER-negative MDA-MB-436 cells. Transfection of the AnxA6 RNAi strongly reduced (~60–80%) the expression of endogenous AnxA6 after 72 h, whereas other annexins, like AnxA2, remained unchanged (data not shown). Downregulation of AnxA6 correlated with a 1.5- to 2.5-fold increase of EGF-stimulated Pan- and H-Ras activity, respectively (Figure 3d). Taken together with previous data from HeLa cells this supports a role for AnxA6 expression levels in p120GAP-mediated Ras inactivation in a variety of cell types (Grewal *et al*., 2005).

Oncogenic Ras is resistant to GAP activity (Downward, 2003; Cook and Lockyer, 2006; Cullen, 2006; Grewal and Enrich, 2006), and to validate that AnxA6 does not inhibit Ras signalling through p120GAP-independent pathways, we determined the effect of AnxA6 overexpression on Ras activity in Hs578T cells, which express oncogenic H-Ras (HRasG12D) (Kraus

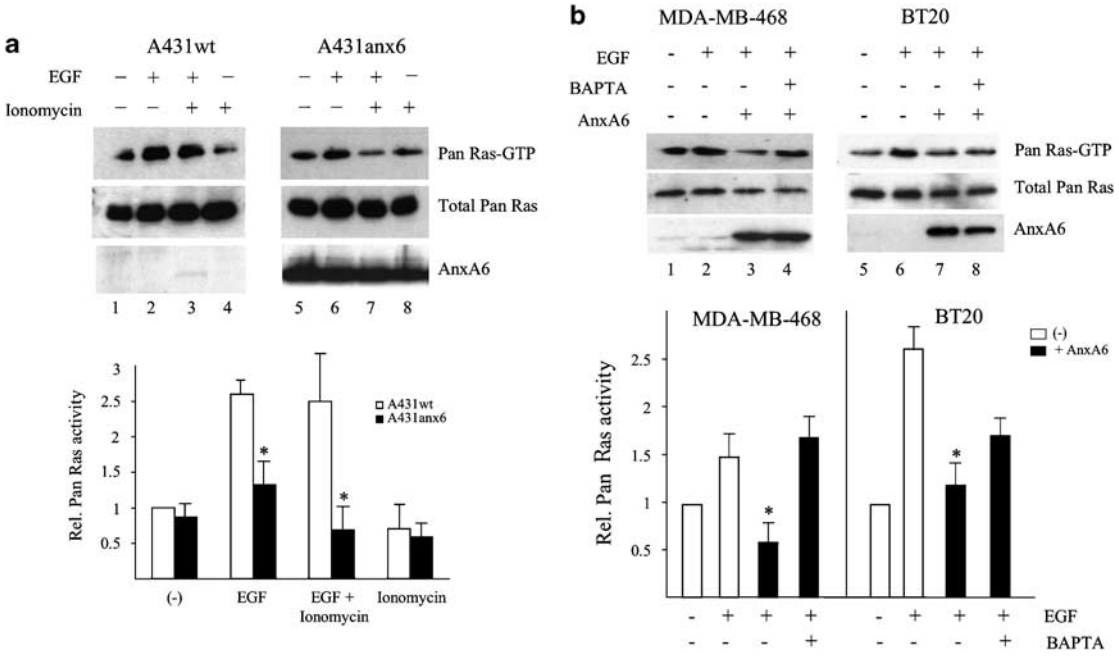

Figure 3 AnxA6 mediates Ca^{2+}-dependent inactivation of Ras activity in EGFR-overexpressing cells. (**a**) A431wt and A431anx6 cells were starved ON and pre-incubated with Ionomycin (2.5 μM) for 2 min. Then cells were incubated ± EGF (10 ng/ml) as indicated and lysates were subjected to RBD pulldowns to determine activated Pan Ras-GTP levels. Total Pan Ras in each lysate is shown. Western blots of three independent Ras activation experiments were quantified and normalized to the amounts of Total Pan Ras. The mean values (± s.d.) are shown. *$P<0.05$ for Student's *t*-test. (**b**) MDA-MB-468 and BT20 cells transfected ± AnxA6 were starved ON, pre-incubated with ± BAPTA-AM (10 μM) for 30 min and treated ± EGF (10 ng/ml) as indicated. AnxA6 expression levels in each lysate are shown. Pan Ras activity was determined as described in (**a**) and western blots of one representative experiment is shown. Three independent experiments were quantified, normalized to the amounts of Total Pan Ras and the mean values (± s.d.) of the relative Ras activity are shown. *$P<0.05$ for Student's *t*-test. (**c**) ER-negative MDA-MB-436 cells were transfected with empty control (−) or expression vector encoding CAPRI, p120GAP and p120GAPΔC2 as indicated. Then, 24 h after transfection, cells were starved ON and incubated ± EGF (100 ng/ml) for 3 min. Pan Ras and H-Ras activity was determined as described in (**a**). Total Pan Ras, H-Ras, Mek1/2, Erk1/2, Mek and Erk activation (P-Mek1/2, P-Erk1/2), p120GAP and CAPRI expression in each lysate is shown. The mean values (± s.d.) from two independent experiments are given. (**d**) MDA-MB-436 cells were transfected with expression vectors encoding scrambled RNAi (scramble) or RNAi-targeting AnxA6 as indicated. Here, 72 h after transfection cells were starved ON and incubated with ± EGF (100 ng/ml) for 3 min as indicated. Pan Ras and H-Ras activity were determined as described in (**a**) and the mean values (± s.d.) of two independent experiments are shown. (**e**) Hs578T transfected ± empty control vector and AnxA6-YFP were starved ON and pre-incubated with Ionomycin (2 μM) for 2 min. Then cells were incubated ± EGF (100 ng/ml) as indicated and lysates were subjected to RBD pulldowns to determine Pan Ras-GTP and H-Ras GTP levels as described in (**a**). Western blots of one out of two independent Ras activation experiments are shown. The amounts of Total Pan- and H-Ras, endogenous AnxA6 and AnxA6-YFP in the lysate is given.

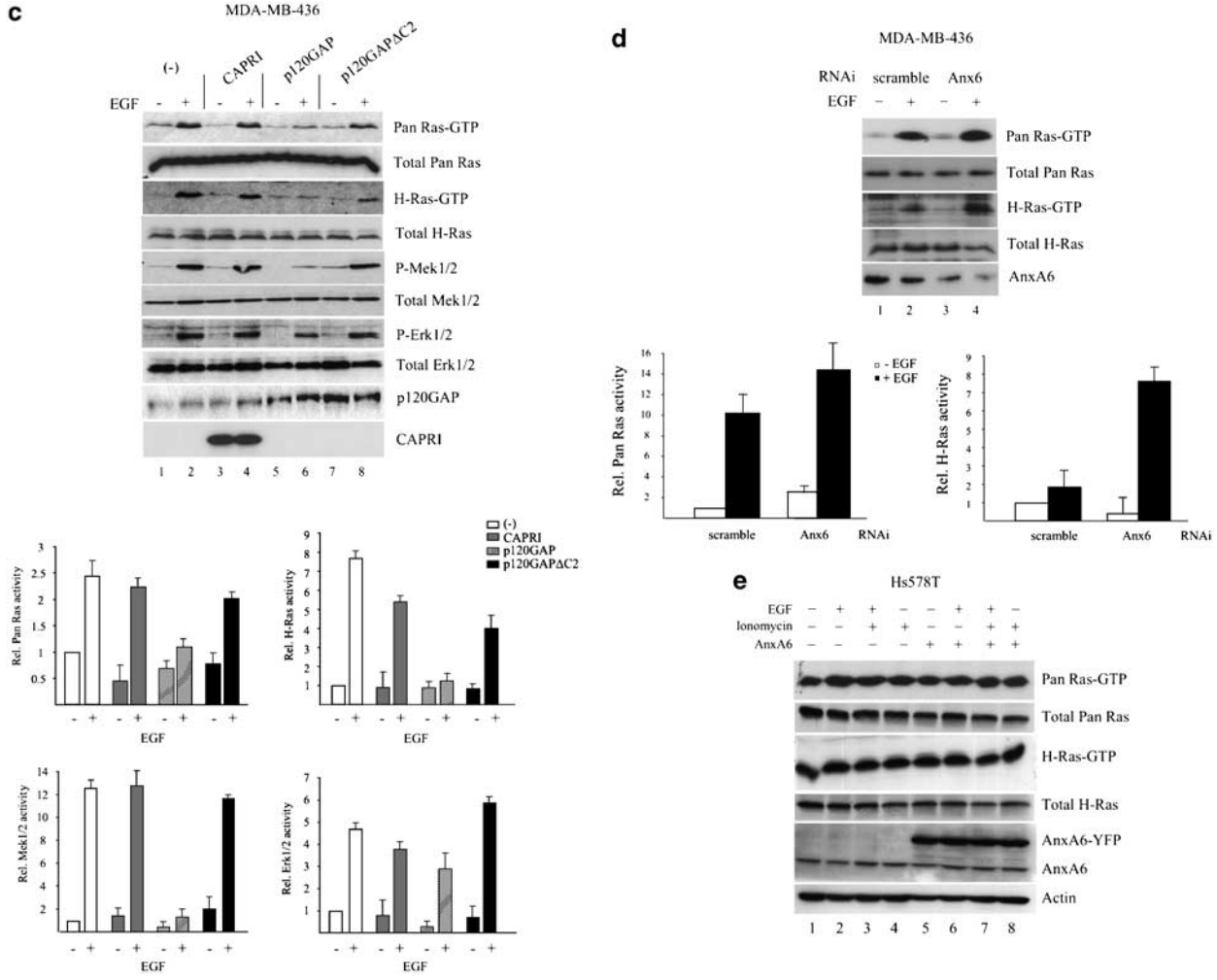

Figure 3 Continued.

et al., 1984) (Figure 3e). Hs578T cells transiently transfected with YFP-tagged AnxA6 were incubated with or without EGF (100 ng/ml) and Ionomycin (2 μM) as described above, and cell lysates were analysed for Pan Ras and H-Ras activity in RBD pulldown experiments. As expected, Hs578T cells are characterized by strongly elevated Pan Ras- and H-Ras-GTP levels even in the absence of EGF (lane 1). Incubation with EGF ± Ionomycin did not affect Ras activity in these cells (lanes 2–4). Importantly, overexpression of AnxA6 did not reduce Pan Ras or H-Ras-GTP levels under any of the conditions tested (Figure 3e, lanes 5–8). Similarly, Mek1/2 and Erk1/2 phosphorylation was not reduced in Hs578T ectopically expressing AnxA6 (data not shown). To complement this, RNAi-mediated knockdown of AnxA6 did not increase basal Ras and MAPK activity in Hs578T (data not shown), altogether supporting a model whereby AnxA6 inhibits Ras in a p120GAP-dependent manner.

AnxA6 inhibits EGF-induced cyclin D1 expression and cell growth in EGFR-overexpressing BCCs

Overexpression of AnxA6 reduces serum-induced cell growth in A431 cells (Theobald *et al*., 1994, 1995). To investigate if this could be linked to the AnxA6-mediated inhibition of the Ras/MAPK pathway, we determined the levels of the cell cycle regulator cyclin D1, a downstream target of Erk1/2 (Figure 4a). In BT20 controls, cyclin D1 levels continued to increase for up to 8 h in the presence of EGF. In the EGF-stimulated BT20anx6 cell line, there was a much less prominent increase in cyclin D1 expression. Similarly, EGF-induced cyclin D1 levels continuously increased in A431wt, but not in A431anx6 (data not shown). Thus overexpression of AnxA6 delays cyclin D1 induction in EGFR-overexpressing cells, such as BT20 and A431.

Consequently, and in agreement with previous data (Theobald *et al*., 1994) clonogenic growth of EGF-incubated A431anx6 cells was reduced significantly compared with controls ($P<0.01$; Figure 4b). We then determined the ability of EGFR-overexpressing MDA-MB-468 ± AnxA6 cells to form colonies and grow in soft agar. MDA-MB-468 and MDA-MB-468anx6 were resuspended in agar containing 10% (v/v) fetal calf serum (FCS) and 100 ng/ml EGF (Timpson *et al*., 2007) and incubated for 21 days (Figure 4c). These experiments showed an ~70% less colonies in the MDA-MB-

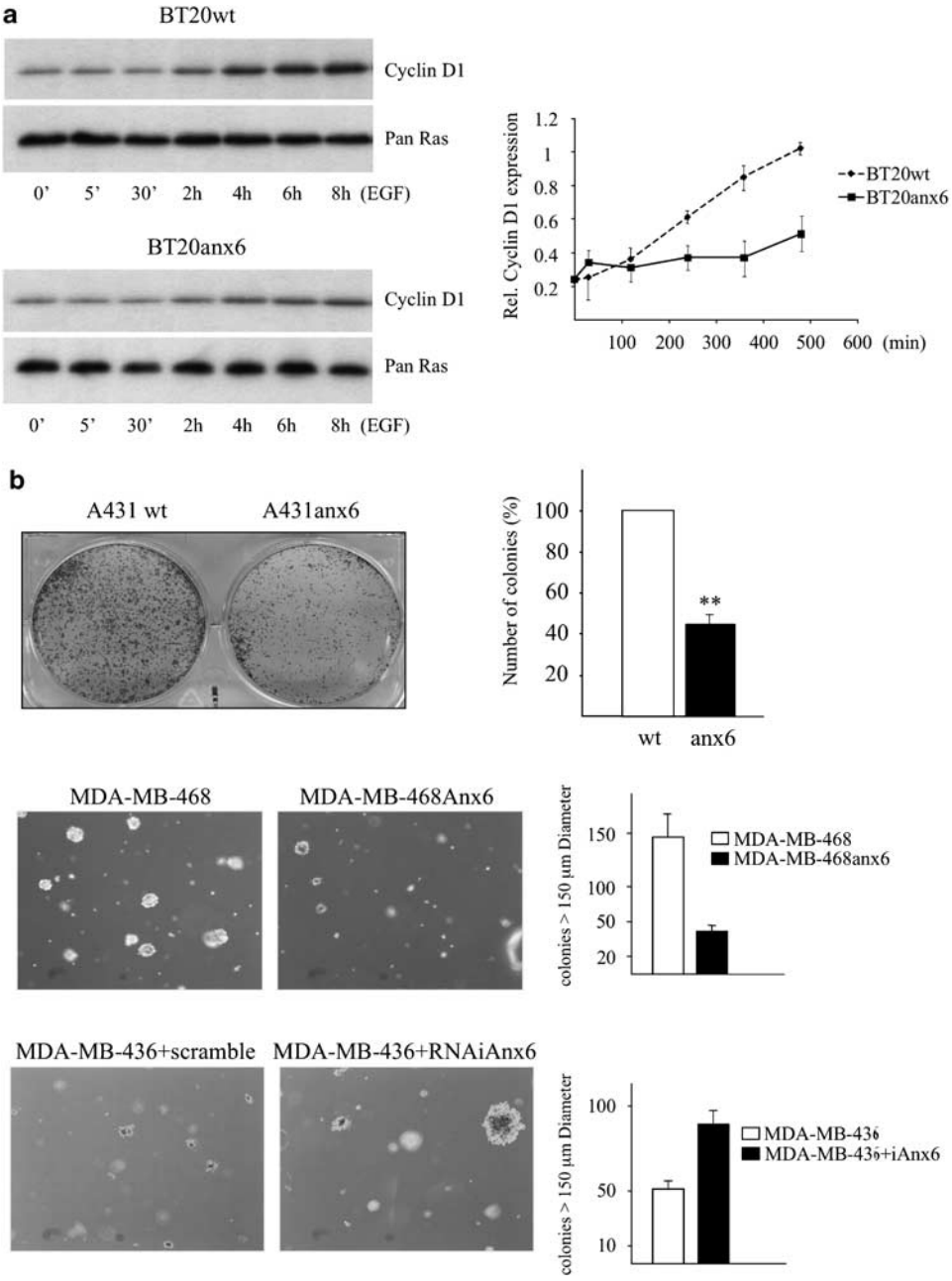

Figure 4 Overexpression of AnxA6 reduces cyclin D1 expression and cell growth in EGFR overexpressing and ER-negative BCCs. (**a**) BT20 wildtype (BT20wt) and BT20 stably expressing AnxA6 (BT20anx6) were starved overnight and treated with EGF (10 ng/ml) for 0–8 h as indicated. Cell lysates were analysed for the amounts of cyclin D1. Western blots of two independent experiments were quantified and normalized to the amounts of Total Pan Ras. (**b**) For colony-forming assays A431 and A431anx6 cells were plated in 6-well plates ($0.6–1.2 \times 10^3$ cells per well) and grown in DMEM, 0.1% fetal calf serum (FCS) and 10 ng/ml EGF, observed two times weekly, fixed and stained as described in Materials and methods. A representative image from two independent experiments with triplicate samples is shown. Colonies containing greater than ~40 cells were quantified using ImageJ software. The number of colonies (%) of the value for control cells (designated as 100%) (± s.d) is given. $^{**}P<0.01$ for Student's *t*-test. (**c**) For anchorage-independent growth assays MDA-MB-468, MDA-MB-468anx6, MDA-MB-436 + scramble and MDA-MB-436 + RNAiAnx6 were grown in soft agar in the presence of 10% (v/v) fetal calf serum (FCS) and EGF (100 ng/ml). All assays were performed in triplicate and cells were scored after 21 days. Colonies greater that 150 µm in diameter were counted and mean values (± s.d) are given.

468anx6 cell line compared with controls. Finally, and in agreement with elevated Ras activity upon AnxA6 knockdown (Figure 3d), AnxA6 depletion in ER-negative MDA-MB-436 increased the number of colonies almost 2-fold in anchorage-independent growth assays (Figure 4c). Thus elevation of AnxA6 reduces the characteristic ability of transformed cells to grow in an anchorage-independent manner, whereas downregulation of AnxA6 increases transformation efficiency.

AnxA6 interacts with active H-Ras in an EGF- and Ca^{2+}-inducible manner

We then addressed the hypothesis that AnxA6 might be associated with H-Ras containing protein complexes, possibly in an EGF- and Ca^{2+}-dependent manner. A431anx6 cells were transfected with H-Ras stimulated ± EGF or Ionomycin, fixed and analysed by immunofluorescence microscopy (Figure 5A). In unstimulated cells AnxA6 is predominantly cytosolic and does not colocalize with H-Ras (panels a–c). In contrast, EGF and Ca^{2+} stimulation resulted in a colocalization of AnxA6 and H-Ras at the plasma membrane (see arrows in Figure 5A, panels d–e and g–h). Similar results were obtained in EGF- or Ionomycin-stimulated A431wt and COS-1 cells transfected with CFP-tagged AnxA6 and YFP-tagged H-Ras (data not shown).

Then co-immunoprecipitations in A431anx6 cells ± EGF were performed (Figure 5B). As shown previously p120GAP co-immunoprecipitates with AnxA6 in both unstimulated and EGF-treated cells (lane 5). In support of AnxA6 interacting with H-Ras, AnxA6 co-immunoprecipitated Ras in EGF-stimulated cells, but not in unstimulated controls (lane 3). Vice versa, AnxA6 was present only in H-Ras immunoprecipitates from EGF-stimulated cells (lane 6).

To confirm AnxA6 interaction with active H-Ras in EGF-activated cells, we performed fluorescence resonance energy transfer (FRET) microscopy experiments

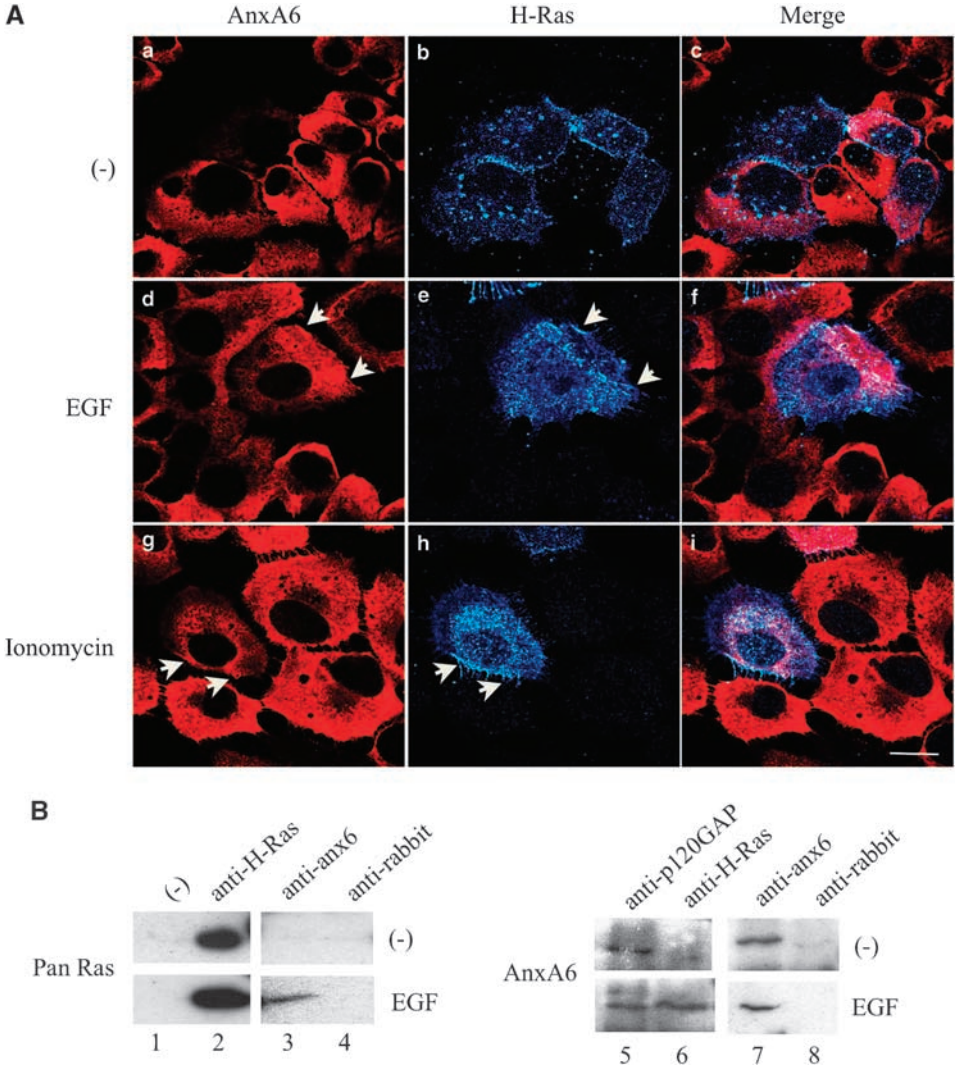

Figure 5 AnxA6 interacts with protein complexes containing active H-Ras. (**A**) A431anx6 cells were transfected with H-Ras. Here, 24 h after transfection, cells were starved ON and incubated ± EGF (10 ng/ml) or Ionomycin (2 μM) for 3 min as indicated. Cells were fixed, immunolabelled with anti-anx6 (red; panels a, d, g) and anti-Pan Ras (blue; panels b, e, h) and analysed by confocal microscopy. The merged images (c, f, i) show a colocalization (white) of AnxA6 and H-Ras in EGF- and Ionomycin-stimulated cells (arrows in d–e and g–h), respectively. Bar is 10 μm. (**B**) Cell lysates (lanes 1–8) from A431anx6 cells incubated ± EGF (10 ng/ml for 3 min) were immunoprecipitated with a rabbit polyclonal antibody against H-Ras (anti-H-Ras; lanes 2, 6), AnxA6 (anti-anx6; lanes 3, 7) p120GAP (anti-p120GAP; lane 5), control rabbit antibody (anti-rabbit; lane 8) or without antibody (−) as indicated and analysed for Pan Ras and AnxA6 by western blotting.

(Figure 6). COS-1 cells were cotransfected with AnxA6-CFP and YFP-HRas and treated ± Ionomycin. CFP, YFP and FRET measurements were initially based on the sensitized emission method (Moreto *et al*., 2008). After background subtraction, correction for spectral bleed through and cross excitation, only background FRET signals (2%) were detected in untreated cells (Figure 6A, panels a–c). In contrast, mean FRET values of Ionomycin-treated cells revealed a Ca^{2+}-inducible interaction (10.5-fold) of AnxA6 and H-Ras (Figure 6A, see white arrows in panel f) at the plasma membrane and possibly endosomal compartments (red arrows, panel f).

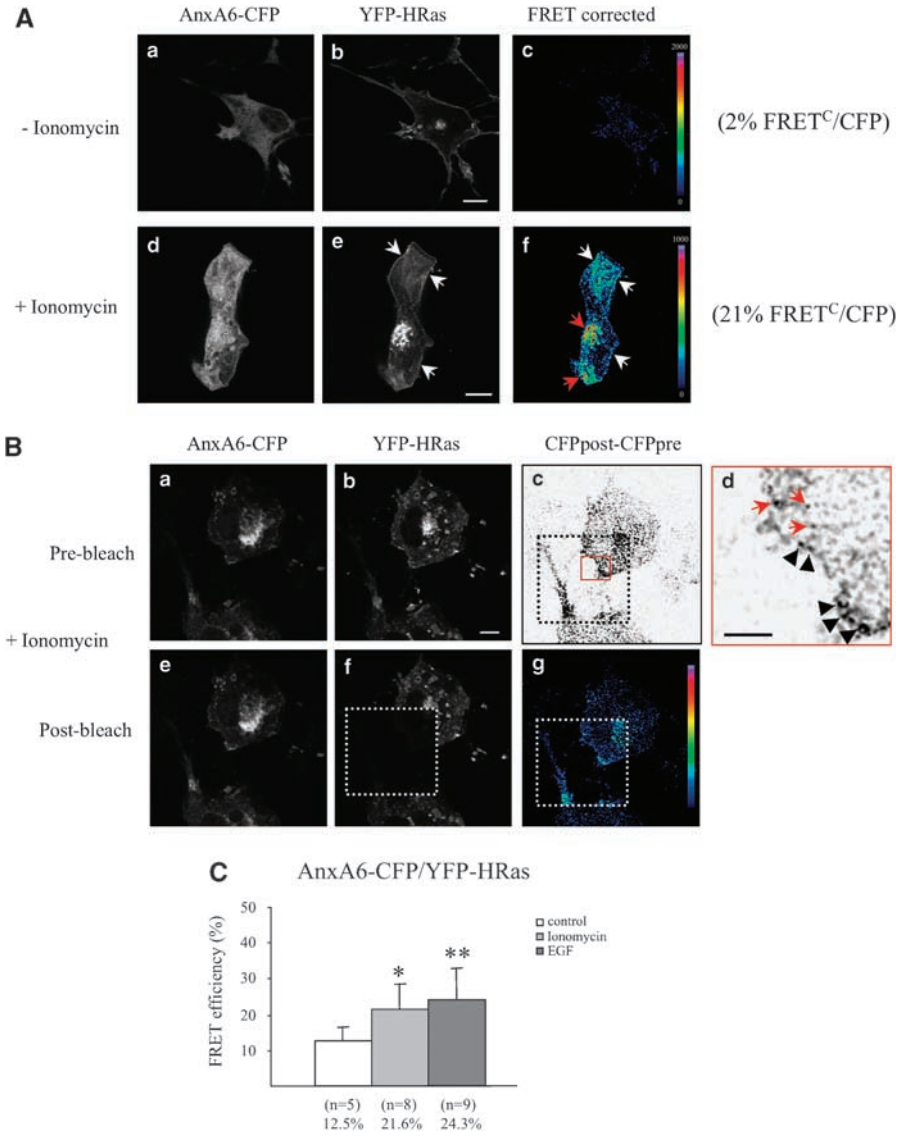

Figure 6 FRET analysis of AnxA6 and H-Ras. (**A**) COS-1 cells were grown in glass coverslips and cotransfected with Anx6-CFP and YFP-HRas. After serum starvation, cells were treated with (+) (panel d–f) or without (−) (panel a–c) 1 μM Ionomycin for 2 min as indicated. Cells were fixed and images were acquired with a Leica TCS SL laser scanning confocal spectral microscope. CFP and YFP channels are shown in panels a, d and b, e, respectively. FRET measurements were based on the sensitized emission method (see Materials and methods for details) and $FRET^C$ (FRET corrected) is presented as a quantitative pseudocolor image (panels c and f). White arrows point to the plasma membrane and red arrows to intracellular labelling. Bar is 10 μm. (**B**) COS-1 cells were grown in glass coverslips, cotransfected with AnxA6-CFP (panels a, e) and YFP-HRas (panels b, f) and treated ± 1 μM Ionomycin, 100 ng/ml EGF (not shown) for 2 min. Representative images of Ionomycin-treated cells are shown (quantification see **C**). After fixation, samples were subjected to FRET image analysis based on the acceptor photobleaching method. Bleached areas are indicated by the dotted square (panels c, f, g). CFP and YFP emission signals were captured before and after photobleaching. FRET efficiency was quantified as the relative increase in CFP emission following YFP photobleaching (see CFPpost-CFPpre, panels c, g). Bar in panel b is 10 μm, as in panels a, c and e–g. An enlarged section of the bleached area in panel c, red square, is shown in panel d. FRET was detected at the plasma membrane (black arrowheads) and in intracellular structures (red arrows). Bar is 3 μm. (**C**) Quantification shows FRET efficiency (%) in control, Ionomycin (1 μM) and EGF (100 ng/ml) treated cells. The number of cells (n) analysed are given in brackets. A significant increase of CFP fluorescence in Ionomycin and EGF-treated cells (* and ** $P<0.05$ and $P<0.01$ for Student's *t*-test, respectively) was observed following YFP photobleaching. For detailed explanation see Materials and methods.

We then determined FRET with an independent approach, FRET acceptor photobleaching (Karpova *et al*., 2003) (Figure 6B). Again, FRET efficiency in non-stimulated cells between Anx6-CFP and YFP-HRas was not above background levels (12.5%), but increased approximately 2-fold after stimulation with Ionomycin and EGF respectively (for quantification see Figure 6C). Similar to the results shown in Figure 6A, FRET was detected at the plasma membrane (black arrowheads, panel d in inserts of Figures 6B and 7A), but also in punctuate vesicular structures (red arrows, Figures 6A, B and 7A).

As these findings indicated binding of AnxA6 only to active H-Ras, we determined FRET efficiency in COS-1 cells cotransfected with AnxA6-CFP and active Ras (YFP-HRasG12V) or inactive Ras (YFP-HRasS17N). High FRET efficiency was detected for AnxA6 only together with H-RasG12 V (26.3–40.1%), but not HRasS17N (2.7–9.1%) under all conditions tested (Figures 7A and B). In fact, AnxA6-HRasG12V interaction was already elevated in unstimulated COS-1 cells compared with wild-type H-Ras (compare quantification of controls in Figures 6C and 7C) and increased even further upon EGF- and Ionomycin-stimulation (Figure 7C). In contrast, FRET did not raise above background $\pm Ca^{2+}$ or EGF in AnxA6-CFP and YFP-HRasS17N cotransfected cells (Figure 7B, for quantification see Figure 7C). These results suggest that AnxA6, possibly together with p120GAP, associates with active H-Ras in EGF-stimulated cells to increase and stabilize H-Ras/p120GAP assembly and downregulate the EGFR/Ras/MAPK pathway.

Discussion

In this study, we demonstrated that AnxA6 is downregulated in EGFR-overexpressing BCCs. In support of AnxA6 promoting Ras/p120GAP assembly, AnxA6 associates with active, but not inactive H-Ras in a Ca^{2+}- and EGF-dependent manner. Restoration of AnxA6 expression increases p120GAP membrane targeting and downregulates Ras signalling and cyclin D1 expression. Importantly, elevation of AnxA6 reduces the anchorage-independent growth of transformed cells whereas downregulation of AnxA6 increases transformation efficiency. Hence in EGFR-overexpressing cells, AnxA6 could be a tumor suppressor to reduce the transforming activity of hyperactive Ras.

It is well known that elevation of Ca^{2+} influences cell proliferation (Jin *et al*., 2007). Characterization of GEFs and GAPs have established the link between Ca^{2+} and Ras signalling and most RasGEFs and RasGAPs are regulated directly or indirectly by Ca^{2+} and/or diacylglycerol (Cullen and Lockyer, 2002; Cook and Lockyer, 2006; Cullen, 2006; Grewal and Enrich, 2006). We propose that expression levels of the Ca^{2+} sensor, AnxA6, determine the contribution of p120GAP in EGFR/Ras inactivation. In unstimulated cells, cytosolic AnxA6 constitutively bind to p120GAP. EGFR activation increases intracellular Ca^{2+}, which promotes the AnxA6-induced targeting of p120GAP to Ras-GTP at the plasma membrane, followed by Ras/p120GAP assembly and Ras inactivation. EGFR, Ras-GTP, p120GAP and AnxA6 containing complexes are then endocytosed through clathrin-coated pits. To ensure Ras inactivation, AnxA6 might stabilize H-Ras/p120GAP complexes in early endosomes. Finally, AnxA6 and p120GAP would be released into the cytosol, whereas H-Ras is recycled to the plasma membrane. Scaffolding proteins, including caveolin, Sur-8, galectin-1 and -3, interact with Ras, might facilitate selective concentration of Ras into discrete microdomains to increase the efficiency and specificity of signalling events (Plowman and Hancock, 2005). The immobilization of EGF-induced active H-, K-Ras and the C-terminal catalytic domain of p120GAP (GAP334) (Murakoshi *et al*., 2004) suggest that Ras/p120GAP complexes are stabilized to increase the efficiency of Ras inactivation. Given that GAP334 is 20 times less active than full-length p120GAP and has a 4-fold lower affinity for Ras (Gideon *et al*., 1992), one can speculate that AnxA6 simultaneously binding to CaLB/C2 and H-Ras allows p120GAP membrane targeting but also immobilization of Ras-GTP for Ras inactivation. Interestingly, we recently demonstrated that high AnxA6 levels reduce the number of caveolae (Cubells *et al*., 2007). As active H-Ras moves out of lipid rafts/caveolae (Plowman and Hancock, 2005) and p120GAP is probably targeted to phospholipid-rich non-raft membrane regions (Murakoshi *et al*., 2004), the dual effects of AnxA6 on p120GAP membrane targeting and caveolae formation could have synergistic effects to inhibit H-Ras in AnxA6-expressing cells.

The relative amounts of scaffolds like IQGAP1, KSR and CNK are known to impact on signal output (Kolch, 2005; Grewal *et al*., 2006; Sacks, 2006). Increasing levels of AnxA6 would therefore be expected to increase p120GAP membrane targeting and Ras inactivation. Scaffold levels can be regulated transcriptionally or translationally, or by their sequestration in specific cellular compartments. AnxA6 could be targeted to different locations, which would allow EGFR/Ras inhibition at multiple locations along the endocytic pathway. In addition, differential expression of AnxA6 could contribute to create signal specificity (Grewal and Enrich, 2006). The downregulation of AnxA6 in EGFR overexpressing and several ER-negative BCCs could be indicative that AnxA6 could have a scaffolding function in some, but probably not all cell types.

Ras GAPs have always been considered as potential tumor suppressors (Bernards and Settleman, 2005) and specific GAPs might inactivate Ras in different cell types. In support of a differential and cell-specific regulation of GAPs, overexpression of p120GAP, but not CAPRI, inhibits EGFR-induced Ras signalling in ER-negative MDA-MB-436 cells. Thus inhibition of Ras-specific GAPs could be a general mechanism to provoke oncogenic activity and carcinogenesis through hyperactive Ras. Out of the GAP family, only Neurofibromin is yet a well-established tumour suppressor. More recently, RNAi screens showed that downregulation

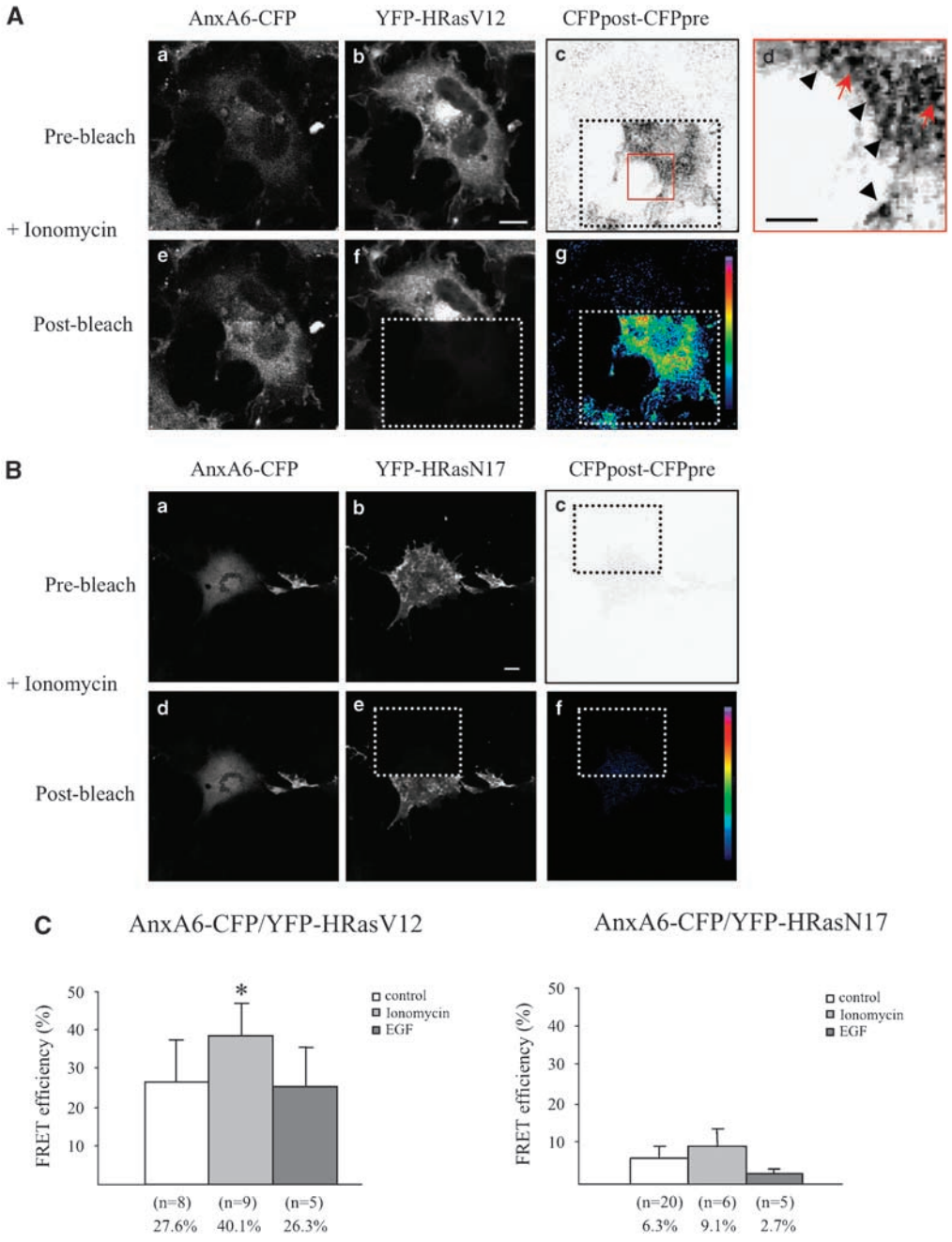

Figure 7 FRET analysis of COS-1 cells cotransfected with AnxA6 and H-RasG12 V or HRasS17N. (**A** + **B**) COS-1 cells were grown in glass coverslips, cotransfected with AnxA6-CFP together with YFP-HRasG12V (**A**) or YFP-HRasS17N (**B**) and treated ± 1 μM Ionomycin or 100 ng/ml EGF (not shown) for 2 min. Representative images of Ionomycin-treated cells are shown (for quantification see **C**). After fixation, samples were subjected to FRET image analysis based on the acceptor photobleaching method as described in Figures 6b and c. Bar is 10 μm (panels a–c and e–g in (**A**) and a–f in (**B**)). FRET was detected in AnxA6 and HRasG12V cotransfected cells at the plasma membrane (black arrowheads, panel d in (**A**)) and in intracellular structures (red arrows). Bar is 4 μm in panel d in (A). FRET was not detectable in cells cotransfected with AnxA6 and HRasS17N (see panels c and f in (B)). (**C**) Histogram showing FRET efficiency (%) of cells cotransfected with AnxA6-CFP and YFP-HRasG12V (**A**) or YFP-HRasS17N (**B**) and treated without (control) or with Ionomycin (1 μM) or EGF (100 ng/ml) for 2 min. The number of cells (*n*) analysed are given in brackets. A significant FRET efficiency was measured in Ionomycin-treated cells cotransfected with AnxA6-CFP and YFP-HRasG12 V (40.1%; $*P<0.05$ for Student's *t*-test). FRET efficiency in cells cotransfected with AnxA6-CFP and YFP-HRasS17N was not above background. For detailed explanation see Materials and methods.

of RASAL- and CAPRI-induced cellular transformation (Kolfschoten *et al*., 2005; Westbrook *et al*., 2005). RASAL is downregulated in multiple tumours by epigenetic silencing (Jin *et al*., 2007). Similarly the Ras-GAP DAB2IP is silenced in different tumours through CpG methylation (Wang *et al*., 2002). Heterozygous mutations in the p120GAP gene have now been associated with abnormal angiogenic remodelling and

capillary-artheriovenous malformation (Boon *et al*., 2005). Deregulation or loss of Ras-specific GAPs may therefore result in aberrant Ras activation and tumorigenesis. Epigenetic silencing of RasGAPs may be a widespread feature in a variety of tumours that carry hyperactive Ras.

Epigenetic silencing of AnxA1 and AnxA2 (Chetcuti *et al*., 2001; Vishwanatha *et al*., 2004) also appears to be common in cancer tissues. Loss of AnxA7 is a marker for prostate cancer and loss of AnxA7 heterozygosity has been observed in ER-negative breast carcinomas (Leighton *et al*., 2004). Along these lines, we identified by bisulfite allelic sequencing that the CpG-rich AnxA6 promoter is heavily methylated only in cells with low AnxA6 levels, such as EGFR-overexpressing A431 and MDA-MB-468 cells (Grewal T, Enrich C and Hitchins M, unpublished results). In addition, AnxA6 is located on chromosome 5q32–q34 and several studies showed a statistically significant loss of 5q31–q35 in ER-negative tumours and its association with ErbB2 amplification (Loo *et al*., 2004; Johannsdottir *et al*., 2006; Pierga *et al*., 2007). Taken together AnxA6 seems to affect cell growth only in the context of co-operating genetic lesions, or in certain susceptible cell types. Down-regulation of AnxA6 is linked to enhanced Ras signalling in EGFR overexpressing and ER-negative cells and restoration of AnxA6-mediated Ras/p120GAP assembly could contribute to decrease hyperactive Ras activity in these cells.

Finally, it should be noted that alternative splicing generating two isoforms of AnxA6 (AnxA6-1 and AnxA6-2) complicate the understanding of AnxA6 functions (Davies *et al*., 1989; Moss and Crumpton, 1990). Although AnxA6-1 is predominantly expressed in normal cells and tissues, AnxA6-2 appears more abundant in some transformed cell lines (Edwards and Moss, 1995). EGF-dependent Ca^{2+} influx in A431 cells is specifically inhibited by AnxA6-1 whereas the AnxA6-2 variant has no effect on cellular phenotype and growth rate (Fleet *et al*., 1999). Although AnxA6-2 has a higher affinity for Ca^{2+}, lower hydrophobicity and lower negative surface charge (Strzelecka-Kiliszek *et al*., 2008), the relationship between expression levels of AnxA6 isoforms and cellular transformation is yet unknown.

Materials and methods

Reagents and antibodies

DMEM, RPMI-1640, geneticin (G418), glutathione, mouse receptor-grade EGF, 2-mercaptoethanol, Ionomycin and BAPTA-AM were from Sigma (Madrid, Spain). Insulin was from Novo Nordisc (Princeton, NJ, USA). Glutathione agarose beads and Protein G sepharose were from Amersham Pharmacia Biotech (Little Chalfont, Buckinghamshire, UK). Expression vectors encoding p120GAP, p120GAPΔC2, CA-PRI, H-Ras, H-RasG12V and HRasS17N were kindly provided by Peter J Lockyer (Cambridge, UK), Michael F Moran (Toronto, Canada) and John F Hancock (Brisbane, Australia), respectively. For the construction of YFP-tagged H-Ras, H-RasG12V and HRasS17N (human), their respective full-length cDNAs were PCR amplified and cloned into pEYFP-C1. For the construction of AnxA6-CFP, AnxA6-YFP, the fluorescent tags were cloned C-terminal of AnxA6 (rat) into pcDNA3.1 (Clontech, Palo Alto, CA, USA). The cloning of the expression vectors for the 1083 and 524 bp *Hin*dIII-*Kpn*I ($Anx6_{1-352}$) and *Hin*dIII-*Asp*1 ($Anx6_{1-175}$) AnxA6 fragments have been described (Pons *et al*., 2001a, b). The A85K mutant RBD protein fused to Glutathione-*S*-Transferase (GST-A85K-RBD) was expressed in the *Escherichia coli* strain BL21 pLysE and purified by glutathione sepharose chromatography as described (Grewal *et al*., 2005). Rabbit anti-H-Ras was from Santa Cruz (Santa Cruz, CA, USA). Rabbit and mouse anti-p120GAP, mouse anti-Ras (Anti-Pan Ras; Ab-3), rabbit-anti-actin, rabbit anti-cyclin D1 were from BD Transduction Laboratories (Lexington, KY, USA). Rabbit antibodies against activated Mek1/2 (P-Mek1/2), Erk1/2 (P-Erk1/2), Total Mek1/2 and Total Erk1/2 were from Cell Signalling (Beverly, MA, USA). The rabbit anti-AnxA6 antibody has been described elsewhere (Grewal *et al*., 2000; de Diego *et al*., 2002). Cy3- and Cy5-conjugated secondary antibodies were from Molecular Probes (Eugene, OR, USA) and Jackson ImmunoResearch (Westgrove, PA, USA). Peroxidase-labelled antibodies, SDS–PAGE molecular weight markers were from Bio-Rad (Hercules, CA, USA).

Cell culture

A431wt, A431anx6 and COS-1 were grown in DMEM together with 10% FCS, L-glutamine (2 mM), penicillin (100 U/ml) and streptomycin (100 μg/ml). MDA-MB-468, BT20, MDA-MB-436 and Hs578 T were grown in RPMI-1640 together with Insulin (0.3 U/ml) and FCS, glutamine and antibiotics as described above. For the generation of stable cell lines in MDA-MB-468 and BT20 cell lines cells were transfected with pcDNAanx6, pcDNAanx6_{1-352} and pcDNAAnxA6_{1-175}, respectively, and selected in the presence of 1 mg/ml G418 as described (Grewal *et al*., 2000). After 2 weeks G418-resistant and AnxA6-expressing colonies were identified.

Growth assays

Colony-forming assays in A431 cells were performed as described (Timpson *et al*., 2007). Cells were fixed stained with Diff Quick stain (Lab Aids, Narrabeen, New South Wales, Australia) and images were captured using a Leica DFC280 camera with Leica Firecam software (version 1.9) and colonies containing greater than approximately 40 cells quantified using the ImageJ software (version 1.34) particle analysis module.

Anchorage-independent growth of MDA-MB-468 and MDA-MB-436 was assayed as recently described (Timpson *et al*., 2007). Cells (1×10^3) were resuspended in RPMI-1640 containing 10% (v/v) FCS, EGF (100 ng/ml) and 0.3% (w/v) agarose (DNA grade, Quantum Scientific, QLD, Australia) and plated on top of an agar layer. The upper layer was allowed to set and was overlaid with 1 ml of media. All assays were performed in triplicate and were incubated for 21 days. Images of colonies were captured as described above and colonies greater that 150 μm in diameter were counted.

RNAi-mediated inhibition of AnxA6 expression

AnxA6 knockdown experiments in MDA-MB-436 were performed with siRNA-targeting human AnxA6 (Pos. 560–579: 5′-GTGGCAGCATACAAAGATG-3′ and Pos. 737–756: 5′-CTGAAATGGGGAACAGATG -3′) cloned into RNAi-Ready pSiren-RetroQ-ZsGreen (Clontech). $1–2 \times 10^6$ MDA-MB-436 cells were transfected with 1.5 μg AnxA6 siRNA

vector and Lipofectamine 2000 (Invitrogen, Carlsbad, CA, USA) according to the manufacturer's instructions. Ras pulldowns and growth assays were conducted 72 h thereafter, when 50–70% of cells expressed the RNAi vector as judged by ZsGreen expression. Control RNAi vector expressing scramble siRNA was used as a negative control.

Measurement of Ras activation
Cells (2×10^6) were pre-incubated ± Ionomycin (2 μM) for 2 min, incubated for 3 min ± 10–100 ng/ml EGF and then the amount of active Ras was determined in Ras pulldown experiments as described (Fridman *et al*., 2000; Grewal *et al*., 2000). Ras-GTP proteins were electrophoresed on 12.5% SDS–PAGE gels, transferred and immunoblotted using anti-Pan Ras or anti-H-Ras antibody.

p120GAP membrane recruitment assay
MDA-MB-468 and BT20 ± AnxA6 were starved overnight, incubated with ± EGF (10 ng/ml) and/or Ionomycin (2 μM) and membrane association of p120GAP and AnxA6, was performed as described (Jaumot and Hancock, 2001; Grewal *et al*., 2005). Here, 100 μg of membranes were incubated with 300 μg of cytosol at 30 °C for 30 min. Membranes were re-isolated by ultracentrifugation and aliquots were analysed by western blotting for p120GAP and AnxA6.

Immunoprecipitation
Immunoprecipitation of H-Ras, AnxA6 and p120GAP were performed as described (Tebar *et al*., 2002; Grewal *et al*., 2005). 500–800 μg of cell lysate was incubated with 2 μg of anti-H-Ras (rabbit), anti-AnxA6 (rabbit), anti-p120GAP (rabbit) or control rabbit antibody for 2 h at 4 °C. After incubation with Protein G sepharose and extensive washing, the immunoprecipitates were analysed for the presence of p120GAP, H-Ras and AnxA6 by western blotting as described (Cubells *et al*., 2007).

Immunofluorescence
A431anx6 cells were grown on coverslips, transfected with H-Ras, activated with EGF (10 ng/ml) or Ionomycin (2 μM) for 3 min, fixed, permeabilized and incubated with first and secondary antibodies as described (Cubells *et al*., 2007, 2008). H-Ras and AnxA6 were visualized using the mouse anti-Pan Ras antibody (BD Biosciences, Erembodegen, Belgium) and rabbit anti-AnxA6 as first and Cy3- and Cy5-donkey anti-mouse (Cy3) and anti-rabbit (Cy5) as secondary antibodies (Jackson ImmunoResearch). Samples were washed extensively and coverslips were mounted with Mowiol. Localization of H-Ras and AnxA6 was studied using an Olympus BX60 microscope and images were collected with IPLab Gel software.

Fluorescence resonance energy transfer
COS-1 cells were transiently transfected with AnxA6-CFP, YFP-HRas, YFP-HRasV12 and YFP-HRasN17. FRET was initially performed by the sensitized emission method as described (Moreto *et al*., 2008). For the FRET acceptor photobleaching method using CFP as donor fluorochrome paired with YFP as acceptor fluorochrome (Karpova *et al*., 2003), a Leica TCS SL laser scanning confocal spectral microscope (Leica Microsystems) equipped with a DMIRE2 inverted microscope, Argon laser and a ×63 oil immersion objective lens (NA 1.32) was used. For visualization of CFP and YFP images were acquired in a line by line sequential mode using 458 and 514 nm laser lines, double dichroic mirror 458/514 nm, emission detection ranges 465–510 and 525–650 nm, respectively, and the confocal pinhole set to 2 Airy units. To minimize the effect of photobleaching, images were collected at low laser intensity. Acceptor photobleaching was performed by irradiating half of the cell in a region of interest (zoom 6.5, pixel size 72 × 72 nm) with the 514 nm laser line set to maximum intensity for six rounds with a line average of two. Under these conditions, 80% of acceptor was bleached. Apparent FRET efficiency (E) was calculated, by normalizing the difference of the donor post- (Ipost) and pre-bleach (Ipre) intensity by the donor post-bleach intensity in the bleached region: E = (Ipost − Ipre /Ipost) 100. As internal negative control, an unbleached region in the same cell was measured. FRET efficiency is expressed as the mean ± s.d. for $n > 5$ cells for each group. Image analysis was performed using the Image Processing Leica Confocal Software (FRET wizard) and ImageJ.

Acknowledgements

We thank Dr Maria Calvo (SCT-UB) for her excellent assistance in confocal microscopy. This study was supported by grants to CE (BFU2006-01151, V-2006-RET2008-0 and fellowship PR-2006-0142 from Ministerio de Educación y Ciencia, Spain) and TG (510293 and 510294 from the National Health and Medical Research Council of Australia and G06S2559 from the National Heart Foundation of Australia). SV is thankful to Ministerio de Educación y Ciencia, Spain, (FPI mobility Program) for a short-term fellowship at the laboratory of TG (Sydney, Australia).

References

Agazie YM, Hayman MJ. (2003). Molecular mechanism for a role of SHP2 in epidermal growth factor receptor signaling. *Mol Cell Biol* **23**: 7875–7886.

Bernards A, Settleman J. (2005). GAPs in growth factor signalling. *Growth Factors* **23**: 143–149.

Blagoev B, Kratchmarova I, Ong SE, Nielsen M, Foster LJ, Mann M. (2003). A proteomics strategy to elucidate functional protein-protein interactions applied to EGF signaling. *Nat Biotechnol* **21**: 315–318.

Boon LM, Mulliken JB, Vikkula M. (2005). RASA1: variable phenotype with capillary and arteriovenous malformations. *Curr Opin Genet Dev* **15**: 265–269.

Chetcuti A, Margan SH, Russell P, Mann S, Millar DS, Clark SJ *et al*. (2001). Loss of annexin II heavy and light chains in prostate cancer and its precursors. *Cancer Res* **61**: 6331–6334.

Chow A, Gawler D. (1999). Mapping the site of interaction between annexin VI and the p120GAP C2 domain. *FEBS Lett* **460**: 166–172.

Cook SJ, Lockyer PJ. (2006). Recent advances in Ca(2+)-dependent Ras regulation and cell proliferation. *Cell Calcium* **39**: 101–112.

Cooper JA, Kashishian A. (1993). *In vivo* binding properties of SH2 domains from GTPase-activating protein and phosphatidylinositol 3-kinase. *Mol Cell Biol* **13**: 1737–1745.

Cubells L, de Muga SV, Tebar F, Bonventre JV, Balsinde J, Pol A *et al*. (2008). Annexin A6-induced inhibition of cytoplasmic phospholipase A2 is linked to caveolin-1 export from the Golgi. *J Biol Chem* **283**: 10174–10183.

Cubells L, Vila de Muga S, Tebar F, Wood P, Evans R, Ingelmo-Torres M *et al*. (2007). Annexin A6-induced alterations in cholesterol transport and caveolin export from the Golgi complex. *Traffic* **8**: 1568–1589.

Cullen PJ. (2006). Decoding complex Ca2+ signals through the modulation of Ras signaling. *Curr Opin Cell Biol* **18**: 157–161.

Cullen PJ, Lockyer PJ. (2002). Integration of calcium and Ras signalling. *Nat Rev Mol Cell Biol* **3**: 339–348.

Daly RJ, Gu H, Parmar J, Malaney S, Lyons RJ, Kairouz R *et al*. (2002). The docking protein Gab2 is overexpressed and estrogen regulated in human breast cancer. *Oncogene* **21**: 5175–5181.

Davies AA, Moss SE, Crompton MR, Jones TA, Spurr NK, Sheer D *et al*. (1989). The gene coding for the p68 calcium-binding protein is localised to bands q32-q34 of human chromosome 5, and to mouse chromosome 11. *Hum Genet* **82**: 234–238.

Davis AJ, Butt JT, Walker JH, Moss SE, Gawler DJ. (1996). The Ca2+-dependent lipid binding domain of P120GAP mediates protein-protein interactions with Ca2+-dependent membrane-binding proteins. Evidence for a direct interaction between annexin VI and P120GAP. *J Biol Chem* **271**: 24333–24336.

de Diego I, Schwartz F, Siegfried H, Dauterstedt P, Heeren J, Beisiegel U *et al*. (2002). Cholesterol modulates the membrane binding and intracellular distribution of annexin 6. *J Biol Chem* **277**: 32187–32194.

deFazio A, Chiew YE, Sini RL, Janes PW, Sutherland RL. (2000). Expression of c-erbB receptors, heregulin and oestrogen receptor in human breast cell lines. *Int J Cancer* **87**: 487–498.

Downward J. (2003). Targeting RAS signalling pathways in cancer therapy. *Nat Rev Cancer* **3**: 11–22.

Edwards HC, Moss SE. (1995). Functional and genetic analysis of annexin VI. *Mol Cell Biochem* **149–150**: 293–299.

Fleet A, Ashworth R, Kubista H, Edwards H, Bolsover S, Mobbs P *et al*. (1999). Inhibition of EGF-dependent calcium influx by annexin VI is splice form-specific. *Biochem Biophys Res Commun* **260**: 540–546.

Fridman M, Maruta H, Gonez J, Walker F, Treutlein H, Zeng J *et al*. (2000). Point mutants of c-raf-1 RBD with elevated binding to v-Ha-Ras. *J Biol Chem* **275**: 30363–30371.

Gawler DJ, Zhang LJ, Reedijk M, Tung PS, Moran MF. (1995). CaLB: a 43 amino acid calcium-dependent membrane/phospholipid binding domain in p120 Ras GTPase-activating protein. *Oncogene* **10**: 817–825.

Gideon P, John J, Frech M, Lautwein A, Clark R, Scheffler JE *et al*. (1992). Mutational and kinetic analyses of the GTPase-activating protein (GAP)-p21 interaction: the C-terminal domain of GAP is not sufficient for full activity. *Mol Cell Biol* **12**: 2050–2056.

Grewal T, Enrich C. (2006). Molecular mechanisms involved in Ras inactivation: the annexin A6-p120GAP complex. *Bioessays* **28**: 1211–1220.

Grewal T, Evans R, Rentero C, Tebar F, Cubells L, de Diego I *et al*. (2005). Annexin A6 stimulates the membrane recruitment of p120GAP to modulate Ras and Raf-1 activity. *Oncogene* **24**: 5809–5820.

Grewal T, Heeren J, Mewawala D, Schnitgerhans T, Wendt D, Salomon G *et al*. (2000). Annexin VI stimulates endocytosis and is involved in the trafficking of low density lipoprotein to the prelysosomal compartment. *J Biol Chem* **275**: 33806–33813.

Grewal T, Tebar F, Pol A, Enrich C. (2006). Involvement of targeting and scaffolding proteins in the regulation of the EGFR/Ras/MAPK pathway in oncogenesis. *Curr Signal Transduct Ther* **1**: 147–167.

Huang DC, Marshall CJ, Hancock JF. (1993). Plasma membrane-targeted ras GTPase-activating protein is a potent suppressor of p21ras function. *Mol Cell Biol* **13**: 2420–2431.

Jaumot M, Hancock JF. (2001). Protein phosphatases 1 and 2A promote Raf-1 activation by regulating 14-3-3 interactions. *Oncogene* **20**: 3949–3958.

Jin H, Wang X, Ying J, Wong AH, Cui Y, Srivastava G *et al*. (2007). Epigenetic silencing of a Ca(2+)-regulated Ras GTPase-activating protein RASAL defines a new mechanism of Ras activation in human cancers. *Proc Natl Acad Sci USA* **104**: 12353–12358.

Johannsdottir HK, Jonsson G, Johannesdottir G, Agnarsson BA, Eerola H, Arason A *et al*. (2006). Chromosome 5 imbalance mapping in breast tumors from BRCA1 and BRCA2 mutation carriers and sporadic breast tumors. *Int J Cancer* **119**: 1052–1060.

Jones RB, Gordus A, Krall JA, MacBeath G. (2006). A quantitative protein interaction network for the ErbB receptors using protein microarrays. *Nature* **439**: 168–174.

Karpova TS, Baumann CT, He L, Wu X, Grammer A, Lipsky P *et al*. (2003). Fluorescence resonance energy transfer from cyan to yellow fluorescent protein detected by acceptor photobleaching using confocal microscopy and a single laser. *J Microsc* **209**: 56–70.

Kolch W. (2005). Coordinating ERK/MAPK signalling through scaffolds and inhibitors. *Nat Rev Mol Cell Biol* **6**: 827–837.

Kolfschoten IG, van Leeuwen B, Berns K, Mullenders J, Beijersbergen RL, Bernards R *et al*. (2005). A genetic screen identifies PITX1 as a suppressor of RAS activity and tumorigenicity. *Cell* **121**: 849–858.

Kraus MH, Yuasa Y, Aaronson SA. (1984). A position 12-activated H-ras oncogene in all HS578T mammary carcinosarcoma cells but not normal mammary cells of the same patient. *Proc Natl Acad Sci USA* **81**: 5384–5388.

Kupzig S, Deaconescu D, Bouyoucef D, Walker SA, Liu Q, Polte CL *et al*. (2006). GAP1 family members constitute bifunctional Ras and Rap GTPase-activating proteins. *J Biol Chem* **281**: 9891–9900.

Leighton X, Srikantan V, Pollard HB, Sukumar S, Srivastava M. (2004). Significant allelic loss of ANX7region (10q21) in hormone receptor negative breast carcinomas. *Cancer Lett* **210**: 239–244.

Lockyer PJ, Kupzig S, Cullen PJ. (2001). CAPRI regulates Ca(2+)-dependent inactivation of the Ras-MAPK pathway. *Curr Biol* **11**: 981–986.

Loo LW, Grove DI, Williams EM, Neal CL, Cousens LA, Schubert EL *et al*. (2004). Array comparative genomic hybridization analysis of genomic alterations in breast cancer subtypes. *Cancer Res* **64**: 8541–8549.

Malaney S, Daly RJ. (2001). The ras signaling pathway in mammary tumorigenesis and metastasis. *J Mammary Gland Biol Neoplasia* **6**: 101–113.

Moreto J, Llado A, Vidal-Quadras M, Calvo M, Pol A, Enrich C *et al*. (2008). Calmodulin modulates H-Ras mediated Raf-1 activation. *Cell Signal* **20**: 1092–1103.

Moss SE, Crumpton MJ. (1990). Alternative splicing gives rise to two forms of the p68 Ca2(+)-binding protein. *FEBS Lett* **261**: 299–302.

Murakoshi H, Iino R, Kobayashi T, Fujiwara T, Ohshima C, Yoshimura A *et al*. (2004). Single-molecule imaging analysis of Ras activation in living cells. *Proc Natl Acad Sci USA* **101**: 7317–7322.

Nori M, Vogel US, Gibbs JB, Weber MJ. (1991). Inhibition of v-src-induced transformation by a GTPase-activating protein. *Mol Cell Biol* **11**: 2812–2818.

Pena V, Hothorn M, Eberth A, Kaschau N, Parret A, Gremer L *et al*. (2008). The C2 domain of SynGAP is essential for stimulation of the Rap GTPase reaction. *EMBO Rep* **9**: 350–355.

Pierga JY, Reis-Filho JS, Cleator SJ, Dexter T, Mackay A, Simpson P *et al*. (2007). Microarray-based comparative genomic hybridisation of breast cancer patients receiving neoadjuvant chemotherapy. *Br J Cancer* **96**: 341–351.

Plowman SJ, Hancock JF. (2005). Ras signaling from plasma membrane and endomembrane microdomains. *Biochim Biophys Acta* **1746**: 274–283.

Pons M, Grewal T, Rius E, Schnitgerhans T, Jackle S, Enrich C. (2001a). Evidence for the Involvement of annexin 6 in the trafficking between the endocytic compartment and lysosomes. *Exp Cell Res* **269**: 13–22.

Pons M, Tebar F, Kirchhoff M, Peiro S, de Diego I, Grewal T *et al*. (2001b). Activation of Raf-1 is defective in annexin 6 overexpressing Chinese hamster ovary cells. *FEBS Lett* **501**: 69–73.

Rentero C, Evans R, Wood P, Tebar F, Vila de Muga S, Cubells L *et al*. (2006). Inhibition of H-Ras and MAPK is compensated by PKC-dependent pathways in annexin A6 expressing cells. *Cell Signal* **18**: 1006–1016.

Rual JF, Venkatesan K, Hao T, Hirozane-Kishikawa T, Dricot A, Li N *et al*. (2005). Towards a proteome-scale map of the human protein–protein interaction network. *Nature* **437**: 1173–1178.

Sacks DB. (2006). The role of scaffold proteins in MEK/ERK signalling. *Biochem Soc Trans* **34**: 833–836.

Smythe E, Smith PD, Jacob SM, Theobald J, Moss SE. (1994). Endocytosis occurs independently of annexin VI in human A431 cells. *J Cell Biol* **124**: 301–306.

Strzelecka-Kiliszek A, Buszewska ME, Podszywalow-Bartnicka P, Pikula S, Otulak K, Buchet R *et al*. (2008). Calcium- and pH-dependent localization of annexin A6 isoforms in Balb/3T3 fibroblasts reflecting their potential participation in vesicular transport. *J Cell Biochem* **104**: 418–434.

Tebar F, Villalonga P, Sorkina T, Agell N, Sorkin A, Enrich C. (2002). Calmodulin regulates intracellular trafficking of epidermal growth factor receptor and the MAPK signaling pathway. *Mol Biol Cell* **13**: 2057–2068.

Theobald J, Hanby A, Patel K, Moss SE. (1995). Annexin VI has tumour-suppressor activity in human A431 squamous epithelial carcinoma cells. *Br J Cancer* **71**: 786–788.

Theobald J, Smith PD, Jacob SM, Moss SE. (1994). Expression of annexin VI in A431 carcinoma cells suppresses proliferation: a possible role for annexin VI in cell growth regulation. *Biochim Biophys Acta* **1223**: 383–390.

Timpson P, Wilson AS, Lehrbach GM, Sutherland RL, Musgrove EA, Daly RJ. (2007). Aberrant expression of cortactin in head and neck squamous cell carcinoma cells is associated with enhanced cell proliferation and resistance to the epidermal growth factor receptor inhibitor gefitinib. *Cancer Res* **67**: 9304–9314.

van der Geer P, Henkemeyer M, Jacks T, Pawson T. (1997). Aberrant Ras regulation and reduced p190 tyrosine phosphorylation in cells lacking p120-Gap. *Mol Cell Biol* **17**: 1840–1847.

Vishwanatha JK, Salazar E, Gopalakrishnan VK. (2004). Absence of annexin I expression in B-cell non-Hodgkin's lymphomas and cell lines. *BMC Cancer* **4**: 8.

Walker SA, Cullen PJ, Taylor JA, Lockyer PJ. (2003). Control of Ras cycling by Ca2+. *FEBS Lett* **546**: 6–10.

Walker SA, Kupzig S, Bouyoucef D, Davies LC, Tsuboi T, Bivona TG *et al*. (2004). Identification of a Ras GTPase-activating protein regulated by receptor-mediated Ca2+ oscillations. *EMBO J* **23**: 1749–1760.

Wang Z, Tung PS, Moran MF. (1996). Association of p120 ras GAP with endocytic components and colocalization with epidermal growth factor (EGF) receptor in response to EGF stimulation. *Cell Growth Differ* **7**: 123–133.

Wang Z, Wilson GF, Griffith LC. (2002). Calcium/calmodulin-dependent protein kinase II phosphorylates and regulates the Drosophila eag potassium channel. *J Biol Chem* **277**: 24022–24029.

Westbrook TF, Martin ES, Schlabach MR, Leng Y, Liang AC, Feng B *et al*. (2005). A genetic screen for candidate tumor suppressors identifies REST. *Cell* **121**: 837–848.

Zhang K, DeClue JE, Vass WC, Papageorge AG, McCormick F, Lowy DR. (1990). Suppression of c-ras transformation by GTPase-activating protein. *Nature* **346**: 754–756.